Protein−Protein Interaction Using Tryptophan Analogues: Novel Spectroscopic Probes for Toxin−Elongation Factor-2 Interactions†

Fouroozan Mohammadi, Gerry A. Prentice, and A. Rod Merrill*

Guelph-Waterloo Centre for Graduate Work in Chemistry and Biochemistry, Department of Chemistry and Biochemistry, University of Guelph, Ontario N1G 2W1, Canada

Received May 21, 2001; Revised Manuscript Received July 5, 2001

ABSTRACT: Previously, we characterized the role of the three naturally occurring Trp residues (W-417, -466, and -558) in the catalytic mechanism of the toxin−enzyme produced by *Pseudomonas aeruginosa* [Beattie and Merrill (1999) *J. Biol. Chem. 274*, 15646−15654]. However, the use of intrinsic Trp fluorescence to study toxin−eEF-2 interaction is inherently limited since the spectral properties of the various Trp residues in both proteins cannot easily be distinguished. To facilitate the study of the protein−protein interaction by Trp fluorescence spectroscopy, the Trp residues in the catalytic domain of exotoxin A were replaced with the amino acid analogues 4-fluorotryptophan, 5-fluorotryptophan, 5-hydroxytryptophan, and 7-azatryptophan. The incorporation of analogues was achieved by using a tightly regulated promoter, *pBAD*, and expressing the protein in a Trp auxotrophic strain of *Escherichia coli*, BL21, in a minimal medium containing the appropriate tryptophan analogue. Quantitative spectral analysis of the analogue-containing proteins using the Decompose program indicated that we had achieved 87−100% incorporation efficiency depending on the Trp analogue being used. Electrospray mass spectrometry analysis verified that we had achieved nearly total replacement of the L-tryptophan residues within the catalytic domain of exotoxin A with the tryptophan analogues 5-fluorotryptophan and 4-fluorotryptophan. The analogue-substituted proteins showed a variation in their catalytic activities with k_{cat} values ranging from 6-fold (4-fluorotryptophan) to 260-fold (5-hydroxytryptophan) lower than the natural enzyme, which was in agreement with previous data using site-directed mutagenesis [Beattie et al. (1996) *Biochemistry 35*, 15134−15142]. However, the analogue-incorporated enzymes did not show any significant change in their ability to bind NAD^+ as substrate, as determined from a fluorescence-binding assay. The spectral properties of the various analogue-incorporated proteins were evaluated and compared with those of the native protein. Furthermore, selective excitation of the 5-hydroxytryptophan-incorporated toxin was exploited to study its interaction with the elongation factor-2 substrate by fluorescence resonance energy transfer to an acceptor chromophore located on the elongation factor-2 protein. The binding between the toxin−enzyme and elongation factor-2 was shown to be independent of the NAD^+ substrate (983 ± 63 nM) and showed a small dependence upon the ionic strength of the solution.

Pseudomonas aeruginosa exotoxin A (ETA)[1] belongs to a family of related bacterial toxins that can be classified according to their protein substrates into four groups: (i) elongation factor-2 ADP-ribosylating toxins (diphtheria and exotoxin A), (ii) heterotrimeric G-protein ADP-ribosylating toxins (cholera and pertussis toxin), (iii) toxins that ADP-ribosylate small GTPases (*Clostridium botulinum* C3 exoenzyme), and (iv) ADP-ribosyltranferases with actin as a substrate (clostridrial ADP-ribosyltransferases, *C. botulinum* C2 toxin, and *Clostrium perfringens* iota toxin). ETA catalyzes the transfer of ADP-ribose from NAD^+ onto elongation factor-2 (eEF-2) and is also a member of the family of enzymes known as mono(ADP-ribosyl) transferases (ADPRT) and specifically is a NAD^+−diphthamide ADP-ribosyltransferase (EC 2.4.2.36). This covalent transfer inactivates eEF-2, rendering it incapable of polypeptide chain elongation, inhibiting protein synthesis, and eventually killing the toxin-infected host cell. The enzyme function of ETA has been localized to domain III (*1*) and includes residues 400−613. Recently, the X-ray crystal structure for domain III complexed with a NAD^+ analogue was reported (*2*).

† Supported by the Canadian Institutes of Health Research (A.R.M.).

* Corresponding author (tel, 519-824-4120 ext 3806; fax, 519-766-1499; e-mail, Merrill@chembio.uoguelph.ca).

[1] Abbreviations: ADPRT, ADP-ribosyltransferase; Amp, ampicillin; 4-FW, 4-fluorotryptophan; 5-FW, 5-fluorotryptophan; 5-HW, 5-hydroxytryptophan; 7-AW, 7-azatryptophan; β-TAD$^+$, β-methylenethiazole-4-carboxamide adenine dinucleotide; Cam, chloramphenicol; 3-D, three-dimensional; DT, diphtheria toxin; ϵ-AMP, 1,N^6-ethenoadenosine 5′-monophosphate; ϵ-ADP, 1,N^6-ethenoadenosine 5′-diphosphate; eEF-2, eukaryotic elongation factor-2; ϵ_M, molar extinction coefficient; ϵ-NAD^+, N^6-etheno-β-nicotinamide adenine dinucleotide; ETA, *Pseudomonas aeruginosa* exotoxin A; FRET, fluorescence resonance energy transfer; GdnHCl, guanidine hydrochloride; HPLC, high-performance liquid chromatography; IAEDANS, 5-[[(acetylamino)ethyl]amino]-naphthalene-1-sulfonic acid; IPTG, isopropyl β-D-thiogalactopyranoside; LINCS, linear combination of basis spectra; MOPS, 3-(*N*-morpholino)-propanesulfonic acid; MWCO, molecular weight cutoff; NAD^+, β-nicotinamide adenine dinucleotide (oxidized form); NATrpA, *N*-acetyltryptophanamide; NATyrA, *N*-acetyltyrosinamide; PE24, *Pseudomonas aeruginosa* exotoxin A 24 kDa C-terminal fragment; SDS−PAGE, sodium dodecyl sulfate−polyacrylamide gel electrophoresis; *t*-Boc, *tert*-butoxycarbonyl; tet, tetracycline; $toxA_C$, portion of the *toxA* gene that encodes domain III; Tris, tris(hydroxymethyl)aminomethane; WT, wild type.

10.1021/bi011035u CCC: $20.00
Published on Web 08/03/2001

The kinetic and stereochemical data indicate that the ADPRT reaction mechanism involves a S_N1 nucleophilic substitution by which the diphthamide residue of eEF-2 attacks the anomeric carbon of ribose, forming a new glycosidic bond between ADP-ribose and diphthamide−eEF-2 (*3*, *4*). The acceptor for the ADPRT reaction is, therefore, the diphthamide residue within eEF-2 (*5*). Kinetic studies indicate that the transfer of the ADP-ribose group from NAD^+ to eEF-2 proceeds through an ordered sequential mechanism where NAD^+ binds first, forming a binary complex that then associates with eEF-2 (*6*, *7*).

It is noteworthy that there is a common fold of approximately 100 residues that contains the NAD^+ binding site that exists for ETA, DT, pertussis toxin, and *Escherichia coli* heat-labile enterotoxin (*2*, *3*, *8*). This 100-residue common fold consists of two antiparallel β-sheets and two α-helices with the active site cleft formed at the interface of the two β-sheets. Interestingly, this NAD^+-binding pocket is seen in ETA (*2*, *8*) and DT (*3*) and represents a new structural motif for binding this nucleotide cofactor that is unique to this family of toxins and is unlike the Rossmann fold that is characteristic of the dehydrogenases. Importantly, this common fold region for ETA and DT is structurally indistinguishable (*3*, *9*).

In this motif, NAD^+ forms a horseshoe-shaped structure that has each end of the molecule projecting into the active site cleft of the C-domain. It makes extensive H-bond and hydrophobic contacts while the phosphate groups at the base of the horseshoe protrude out of the cleft and are exposed to solvent (*3*). Bell and Eisenberg (*3*) recently proposed that the ADPRT enzymes comprise a new class of NAD^+-binding proteins (class 7).

Our research group has been studying the role of the Trp residues (W-417, -466, and -558)[2] within the enzyme domain of ETA in the catalytic mechanism (*4*, *10*). Previously, we were using a crude (50% pure) eEF-2 preparation, but recently we have successfully purified this protein to be employed as an enzyme substrate for ETA (*4*). Wheat germ eEF-2 possesses several Trp residues, and this complicates analysis of fluorescence data for toxin−eEF-2 interactions. However, until only recently, the interaction of proteins such as ETA with another protein that contains Trp residues could not be studied by intrinsic Trp fluorescence methods. Notably, Hogue and Szabo (*11*) reported the incorporation of 5-hydroxytryptophan (5-HW) into the calcium-binding protein, oncomodulin, from rat. Concurrently, Ross and colleagues (*12*) reported the successful incorporation of 5-HW into bacteriophage lambda cI repressor. Subsequently, a comprehensive review describing this approach to the study of protein−protein interactions has been published (*13*).

The power of the approach to employ analogue-incorporated proteins for fluorescence spectroscopic analysis is found in the ability to selectively excite the Trp analogues in the presence of naturally occurring Trp. This is feasible because the absorption spectrum of compounds such as 7-azatryptophan (7-AW) and 5-HW is red shifted, yielding a significant molar extinction coefficient (ϵ_M) at 310−315 nm, where the ϵ_M for L-Trp is near zero. This enables the study of protein−protein interactions by measuring the fluorescence from a Trp analogue in the presence of several naturally occurring Trp residues. For example, Trp analogue incorporation has been used to study the interaction of insulin with its receptor (*14*). Furthermore, employing intrinsic fluorescence to study protein−protein interactions does not suffer from the obvious disadvantages of using extrinsic fluorescence probes, including (1) generation of different conformational states of the labeled protein by the probe, (2) alteration of protein interactions by the probe, and (3) heterogeneity of labeling sites because of difficulties in linking the extrinsic probe to a specific residue or binding the extrinsic probe to an unique site.

In this paper we report the successful incorporation of the Trp analogues 4-fluorotryptophan (4-FW), 5-fluorotryptophan (5-FW), 5-HW, and 7-AW into the catalytic domain of ETA. Careful spectral analysis indicated that we achieved analogue incorporation efficiencies approaching 100% for all but 5-HW, which was incorporated at a level of 85%. We have exploited the 5-HW-incorporated C-terminal catalytic fragment of ETA (PE24) to study the nature of the protein−protein interaction between the toxin and its protein substrate, eEF-2.

EXPERIMENTAL PROCEDURES

Preparation of the PE24 pBAD Construct. The gene encoding PE24 ($toxA_C$) was amplified using Pwo DNA polymerase (Roche Biochemicals, Laval, Quebec) with an N-terminal (forward) primer AAGAATTCCCATGGCCGAAGAAGCTTTCCT and the C-terminal (reverse) primer AATCTAGAAGGCCGGCTCCTGCGAAG. The N-terminal primer introduced the *Eco*RI restriction site, along with additional bases (AT) that are required to precede the site for efficient digestion, prior to the ATG (Met) codon. The C-terminal primer introduced the *Xba*I restriction site, along with additional bases (AA) that are required to precede the site for efficient digestion, just downstream of the stop codon for the truncated *toxA* gene. The PCR product was gel purified and extracted using AgarAce (Promega, Nepean, Ontario) followed by phenol/chloroform extraction and ethanol precipitation. Then, the PCR product was sequentially digested with *Eco*RI and *Xba*I, and the digested DNA fragment was again gel purified as before. The $P_{BAD}22$ vector (kindly provided by Dr. Nancy Martin), which carries Amp^r, M13 origin of replication, araC, $rrnBT_{12}$, and the P_{BAD} promoter, was purified from JM109 cells with a Qiagen 100 tip and then sequentially digested with *Eco*RI and *Xba*I. It was then dephosphorylated with alkaline phosphatase after gel purification. The PCR product was ligated into the multiple cloning site of the $P_{BAD}22$ vector using T4 DNA ligase at 16 °C overnight, followed by incubation of the ligation mixture with competent JM109 cells. The transformants were selected by plating on ampicillin-containing 2×YT medium. Restriction digestion analysis combined with cycle DNA sequencing confirmed the integrity of the construct, *fmpBADPE24*, for protein expression.

Construction of the Tryptophan Auxotroph. (A) Preparation of P1 Lysogens. The Trp auxotroph strain NK7402 [λ^-, *trpB83*: *Tn10*, *IN* (*rrnD-rrnE*) *1*] (*E. coli* Genetic Stock Center, Yale University, New Haven, CT) was grown

[2] The notation W-### designates the Trp mutant C-terminal fragment that possesses a single Trp residue at that designated site (###) according to the numbering of the whole toxin protein sequence. The notation Trp ### refers to the specific Trp residue within the peptide sequence.

overnight in 2 mL of L-broth. The next day, 100 μL of 100 mM $CaCl_2$ was added to the overnight culture, and after thorough mixing, 0.1 mL of the overnight culture was added to 0.1 mL of P1 lysate [P1, a gift from Dr. J. Wood, University of Guelph, carries chloramphenicol (Cam) resistance] for 10 min. The culture was then streaked for single colonies on LB plates containing Cam (25 μg/mL). Next, a single colony was picked and grown overnight at 30 °C in 5 mL of L-broth containing Cam (25 μg/mL).

(B) Preparation of Lysate. The next day, 1 mL of the overnight culture was added to 9 mL of L-broth containing 10 mM $MgSO_4$ in a 125 mL flask. The cells were grown with shaking at 30 °C to an OD_{650} of 0.8. At this time, the temperature was shifted to 42 °C, and the cells were grown for 35 min with shaking. After 35 min, the temperature was shifted to 37 °C for 60 min.

(C) Transduction with P1 Lysates. The recipient strain, BL21 (λDE3), was grown for transduction overnight at 37 °C in 5 mL of LB broth. The cells were then centrifuged (10 min, 10 000 rpm), and the supernatant was decanted. After resuspending the cell pellet in 5 mL of medium, the cells were incubated at 37 °C for 15 min. Next, 100 μL of the suspended cells was added to each of five test tubes. To the first tube, 100 μL of the P1 lysate was added. Tenfold dilutions of the lysate were added to the second, third, and fourth tubes, respectively. Nothing was added to the fifth tube, which served as a control. Finally, in a sixth tube, 100 μL of the lysate was added (no cells) as another control. After incubation of all tubes at room temperature for 20 min, phage adsorption was stopped by the addition of 200 μL of 1 M sodium citrate (pH 7.0) to each tube. LB broth (400 μL) was added to each tube, and the tubes were incubated for 1 h at 30 °C to allow for the expression of the Tet phenotype of the auxotroph. Next, 3 mL of prewarmed top agar (45−50 °C) was added to each tube and plated onto LB plates containing Tet (10 μg/mL). After the agar solidified, the plates were incubated overnight at 37 °C. The colonies (transductants) were streaked onto Tet plates to eliminate any background expression. The transductants were then streaked onto MOPS medium (*15*) in plates containing 1% L-Trp and plates lacking Trp to test for Trp auxotrophy. Transductants [BL21 (λDE3)/NK7402] were rendered competent by the $CaCl_2$ method (*16*).

Overexpression and Purification of PE24. For the expression of analogue-incorporated PE24 (containing a 6-His tag at the C-terminus), the plasmid *fmpBADPE24* (pBAD) or *rmpT7PE24* (T7), which codes for the catalytic domain of ETA (residues 400−613; *8*), was used to transform an *E. coli* lysogenic cell line auxotrophic for L-tryptophan, *FL*BL21 (λDE3), prepared as detailed above. It was determined that the auxotrophic BL21 (λDE3) cells also worked well for the pBAD expression system. One microliter of this plasmid was incubated with competent BL21 (λDE3) cells followed by heat shock treatment (*17*) into and plated onto two 2×YT medium plates containing 100 μg/mL ampicillin (Amp) and incubated overnight at 37 °C. The next day, each plate was scraped into 5 mL of super L-broth containing 2.0% glucose and 100 μg/mL ampicillin, and the cells were grown for 1 h at 37 °C. The 5 mL culture was then transferred to a 500 mL flask containing M63 minimal medium supplemented with 2.0% glucose (repressor), 100 μg/mL ampicillin, 0.25 M L-Trp, and 0.4% glycerol (carbon source). This culture was grown to 0.5−0.7 OD_{650} at 37 °C, after which the cells were harvested by centrifugation at 10000*g* for 10 min and the supernatant was decanted.

The cell pellet was then washed twice with 500 mL of M63 medium supplemented with 0.2% glycerol to remove all traces of residual L-Trp. The cell pellet was then resuspended into the original volume of M63 media containing 0.6% glycerol and 100 μg/mL ampicillin and grown for a further 20 min to deplete any residual tryptophan in the culture. Subsequently, the tryptophan analogues (D,L-forms) (Sigma, St. Louis, MO) were added to the minimal medium at a final concentration of 0.50 mM, and the cells were induced with 1% arabinose (pBAD) or 1 mM IPTG (T7). The culture was allowed to grow for 3 h at 37 °C, and the cells were harvested again by centrifugation at 10000*g* for 10 min. The cell pellets were resuspended and homogenized in 40 mL of binding buffer (5 mM imidazole, 0.5 M NaCl, 20 mM Tris-HCl, pH 7.9) containing DNase (0.0125 mg/mL). The homogenate was lysed in a French pressure cell (twice) at 10 000 psi, and the lysate was centrifuged for 25 min at 17000*g*. The supernatant was decanted and diluted with one-fifth volume of binding buffer and then filtered twice through Whatman no. 1 and once through Whatman no. 2 filter paper. The filtered solution was applied to a 1 mL TALON metal affinity resin column (Clonetech, Palo Alto, CA), previously equilibrated in binding buffer. The column was subsequently washed with 25 mL of binding buffer followed by 20 mL of wash buffer (30 mM imidazole, 0.5 M NaCl, pH 7.9). The proteins were eluted and collected in 1 mL fractions with elution buffer (100 mM imidazole, 0.5 M NaCl, pH 7.9).

The purified PE24 proteins were concentrated and exhaustively dialyzed against 20 mM Tris-HCl and 50 mM NaCl, pH 7.4, buffer and then concentrated to approximately 2 mg/mL with an Amicon Centriprep cencentrator (Amicon Ltd., Danvers, MA) and filtered through a 0.2 μm Acrodisc membrane filter (Gelman Science, Rexdale, ON), and the protein concentration was determined by absorbance using ϵ_{M280} of 2.731×10^4 M^{-1} cm^{-1} (WT) calculated according to the method of Gill and von Hippel (*18*). The proteins were shown to be purified to relative homogeneity by overloading lanes during SDS−PAGE and by Western blotting analysis using the antibody to PE24H and the anti-His antibody (Santa Cruz Biotech Inc., Santa Cruz, CA) as previously described (*20*). The BCA assay (Pierce, Rockford, IL) was used to determine the protein concentration of the spectrally enhanced proteins using the WT PE24 as the protein standard. The proteins were dispensed into small aliquots and frozen at −80 °C.

Purification of eEF-2 from Wheat Germ. eEF-2 was purified from wheat germ (Sigma Chemical Co., St. Louis, MO) as previously described (*4*). The N-terminus of the purified 95 kDa protein, eEF-2, was sequenced from PVDF membrane after electrophoretic transfer as previously described (*10*). The sequence for the protein was NH_2-Val-Lys-Phe-Thr-Ala-Glu-COOH, which indicated that the wheat germ protein is a member of the eEF-2 family of proteins based on sequence alignment with a number of eEF-2 sequences from various species.

Spectroscopic Measurements. Absorbance spectra were obtained at room temperature with a Perkin-Elmer λ-6 double beam, scanning absorption spectrometer (Perkin-Elmer, Nor-

walk, CT) interfaced to a personal computer. All absorbance spectra of proteins and amino acid model compounds were scanned from 250 to 360 nm (2 nm slit width) in 20 mM Tris-HCl buffer and 50 mM NaCl, pH 7.6. Fluorescence emission spectra were recorded on a computer-controlled PTI Alphascan-2 spectrofluoroimeter (Photon Technology Inc., South Brunswick, NJ) attached to a circulating water bath for thermal regulation. Fluorescence emission spectra of native PE24 and analogue-containing PE24 were scanned from 310 to 500 nm (excitation at 295 nm, 4 nm excitation and emission band-passes) and measured in 20 mM Tris-HCl buffer and 50 mM NaCl, pH 7.6 at 25 °C. Wavelength-dependent bias of the optical and detection systems was corrected, and appropriate blanks were subtracted.

Fluorescence-Based ADPRT Assay. Samples were assayed for ADPRT activity by using a newly developed fluorometric assay based on the work of Klebl and Pette (*19*) and developed in our laboratory (*20*). The reaction medium for assessment of ADPRT activity contained 20 mM Tris-HCl, pH 7.4, 0−500 μM 1,N^6-etheno-NAD (ϵ-NAD^+; Sigma, St. Louis, MO), and 14 μM eEF-2 in a total volume of 70 μL in a 3 mm × 3 mm ultramicro quartz cuvette (Hellma Ltd., Mississauga, ON) at 25 °C. After 5 min equilibration time, the reaction was started by the addition of 5 nM native PE24 (final concentration, higher concentrations for the analogue proteins), and the progress of the ADPRT reaction was monitored by excitation at 305 nm with the fluorescence emission measured through a 309 nm cutoff filter (Oriel Corp., Stratford, CT). The ϵ-ADP-ribosyl-eEF-2 produced was quantified by calibration with ϵ-AMP (Sigma, St. Louis, MO), which exhibits the same fluorescence quantum yield as ϵ-ADP-ribose, the fluorescent product attached to eEF-2 (*21*).

Fluorescence Labeling of eEF-2. Purified wheat germ eEF-2 protein was labeled with IAEDANS (Molecular Probes Inc., Eugene, OR) by incubation of 2 mg of protein in reaction buffer (20 mM Tris-HCl, pH 8.0) containing dithiothreitol (DTT, 3:1 mol of DTT:mol of protein) for 30 min followed by the addition of a concentrated stock of IAEDANS (20 mg/mL in DMSO at 10:1 mol of IAEDANS:mol of protein). The reaction mixture was gently mixed on a nutator, and the sulfhydryl labeling reaction was stopped after 10 min at 25 °C by the addition of a 100-fold excess of DTT. The reaction mixture (300 μL) was loaded onto a Bio-Rad Econo-Pac 10DG column (Bio-Rad, Mississauga, ON) equilibrated in 20 mM Tris-HCl and 50 mM NaCl, pH 7.8, and 0.5 mL fractions were collected. The protein−AEDANS adduct eluted from the column in a peak that was completely separated from the free fluorophore peak. The stoichiometry of the labeling reaction was ascertained by determining the eEF-2 concentration using the BCA protein assay with BSA as the standard and by absorption spectroscopy using the molar extinction coefficient (ϵ_{M337} = 6000 M^{-1} cm^{-1}) for AEDANS (*22*).

Fluorescence-Based eEF-2 Binding Assay. To eliminate the fluorescence emission from eEF-2 (eight predicted Trp residues), it was necessary to use the 5-HW−PE24 protein because of the unique spectral properties of 5-HW. The 5-HW analogue possesses a large red-shifted absorption spectrum, which provided the opportunity to excite 5-HW−PE24 at 310 nm, a wavelength where the molar extinction coefficient of eEF-2 is nearly zero (Figure 2B). Accordingly, aliquots of labeled eEF-2 protein were added to 0.5 μM 5-HW-incorporated PE24 (5-HW−PE24) in 20 mM Tris-HCl and 50 mM NaCl, pH 7.8. The fluorescence intensity of 5-HW−PE24 was monitored with a Cary Eclipse fluorometer (Varian, Canada) equipped with a Peltier thermostated multicell holder at 25 °C with excitation at 310 nm (5 nm band-pass) and emission at 360 nm (5 nm band-pass). The raw fluorescence data were corrected for the dilution factor, and the dissociation constant for eEF-2 binding with PE24 was determined using the equation (single binding-site model):

$$\Delta F_i/\Delta F_{max} = \frac{[\text{eEF-2}]}{K_d + [\text{eEF-2}]}$$

where ΔF_i is the change in fluorescence intensity for each ligand (eEF-2) concentration upon macromolecular association, ΔF_{max} is the maximum change in fluorescence intensity at saturation of the ligand-binding site within PE24, and K_d is the dissociation constant for the binding of eEF-2 with PE24.

NAD^+-Binding Measurements. The method for determining the binding constants for spectrally enhanced and native PE24 was essentially as previously described (*4*).

Mass Spectrometry Analysis of PE24. The protein samples were run on a Micromass Quatro II mass spectrometer (Micromass, Manchester, England) fitted with an electrospray source. Flow injection analysis was used with the carrier solvent consisting of 50:50 acetonitrile:water with 0.1% trifluoracetic acid. Approximately 10% methanol was added to the protein samples, which were in distilled water, and 5−10 μL of the sample solution was injected. Each sample required from 8 to 20 scans, and the data were processed using MassLynx Version 2.0 using the Maximum Entropy software supplied with the program in order to generate spectra on the absolute molecular weight scale.

Analysis of Analogue Incorporation Using Absorbance Spectra. To assess the degree of analogue incorporation, the absorption spectra of PE24 analogue proteins were analyzed by deconvolution based on the model compounds *N*-acetyltryptophanamide (NATrpA) and *N*-acetyltyrosinamide (NATyrA) with the appropriate Trp analogue, either 4-FW, 5-FW, 5-HW, or *t*-Boc (α-amino)-7-AW (a gift from Dr. J. B. A. Ross). This was performed by first obtaining basis spectra for these model amino acids in 6 M guanidine hydrochloride (GdnHCl, Sequanal grade; Pierce Chemical Co., Rockford, IL) in 20 mM Tris-HCl and 50 mM NaCl buffer (pH 7.6). The absorbance spectra of 6 M GdnHCl denatured analogue proteins were then fit, between 270 and 350 nm, with the basis set spectra using a fitting program, Decompose 1.03 (written in Visual Basic 4.0 by Uwe Oehler) as described by Waxman et al. (*23*). To avoid overlap with the absorption of phenylalanine residues, the protein spectrum below 270 nm was not used in the fitting routine.

In the Decompose analysis program, individual absorbance spectra were fit to the relationship

$$A_T(\lambda) = \sum a_i A_i(\lambda)$$

where $A_T(\lambda)$ is the absorbance of the protein at each wavelength λ, $A_i(\lambda)$ are the absorbances of the basis spectra, and a_i is the relative molar amount of each basis spectrum

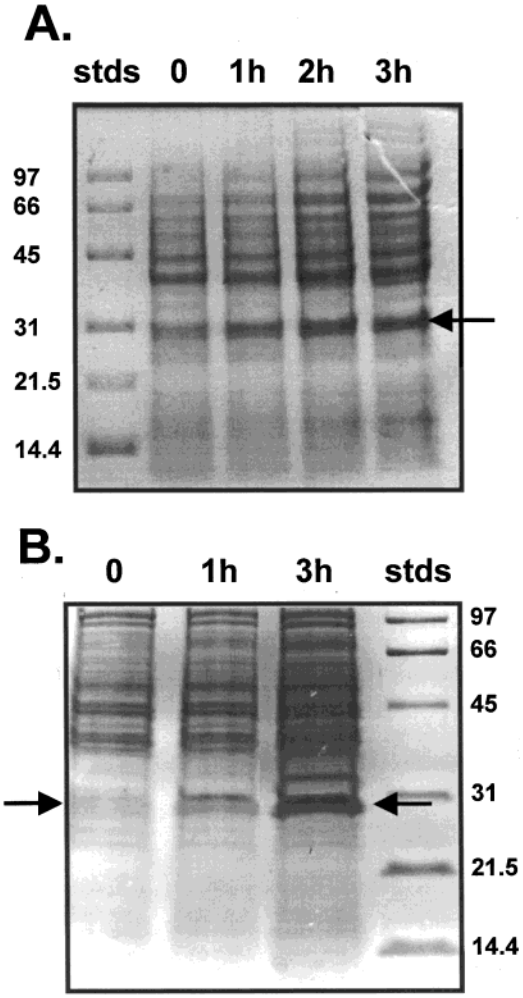

FIGURE 1: Miniprep test for protein expression of 7-AW−PE24 in (A) the T7 expression system and (B) the pBAD expression system. Samples were prepared as described in Experimental Procedures using the BL21(λDE3) expression system (time 0 for both gels corresponds to cells prior to induction) and 1, 2, and 3 h after induction, respectively. Molecular mass standards (Da, top to bottom): phosphorylase *b* (97 400), bovine serum albumin (66 200), ovalbumin (42 699), carbonic anhydrase (31 000), soybean trypsin inhibitor (21 500), and lysozyme (14 400). The arrow indicates the position of the PE24 protein (28 000 Da). The SDS−PAGE gel was stained with Coomasssie brilliant blue.

in the protein spectrum (*12*). The relative molar amounts of each basis spectrum (relative scaling factor) were determined from analysis of the absorbance spectra of two polypeptides, adrenocorticotropin and glucagon, each containing one tryptophan and two tyrosine residues (*21*). The quality of the fit was evaluated by visual inspection and from the residual plots of the fitted data sets.

RESULTS

Overexpression and Production of 7-AW−PE24. The effect of the analogue 7-AW, when present in minimal medium, on the overexpression of PE24 under control of the T7 or the *pBAD* promoter can be seen in panels A and B of Figure 1, respectively. The level of protein expression was reduced when 7-AW was provided as the Trp source in the minimal medium for the L-Trp auxotrophic strain BL21 (λDE3)/NK7402 (data not shown). In Figure 1A there is background expression of PE24 for the T7 system (0 h lane). However, Figure 1B shows that the *pBAD* expression system

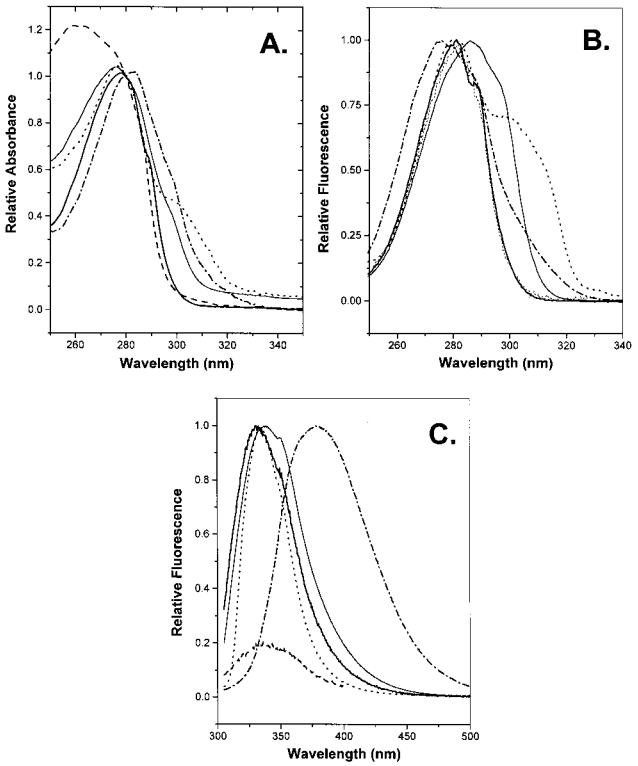

FIGURE 2: Peak normalized (A) absorbance spectra, (B) fluorescence excitation spectra, and (C) fluorescence emission spectra of native PE24 (bold solid line), 4-FW−PE24 (dashed line), 5-FW−PE24 (thin line), 5-HW−PE24 (dotted line), and 7-AW−PE24 (dot-dash line). The proteins were in 20 mM Tris-HCl and 50 mM NaCl, pH 7.8, buffer at 25 °C. The spectral band-passes were 2 nm for absorbance and 4 nm (excitation) and 4 nm (emission) for fluorescence measurements (λ_{ex} = 295 nm). The protein concentrations were 0.25 mg/mL, and the fluorescence spectra were normalized to 1.0 at the λ_{ex}(max) or λ_{em}(max) for the fluorescence excitation and emission spectra, respectively. Other conditions for the experiments were as described in Experimental Procedures.

is more tightly regulated than the T7 system and that expression of PE24 is repressed in the presence of glucose and in the absence of arabinose (0 h lane). This difference in repression between the two promoter systems is partly due to the "gene leakage" that is present in the T7 expression system. Introduction of the *pLysS* plasmid (codes for T4 lysozyme) into the BL21 cells, a known inhibitor of T7 RNA polymerase, caused a total repression of the PE24 production (in the presence of 7-AW) that could not be overcome with IPTG induction. These results motivated us to use the *pBAD* expression system for tryptophan analogue incorporation into PE24 since the basal expression level of PE24 was negligible and protein induction was to a reasonable level (Figure 1B, 3 h lane). Furthermore, the stringent repression seen with the *pBAD* expression system would facilitate higher incorporation efficiency of the tryptophan analogues into the enzyme domain of the toxin.

Analogue Incorporation Efficiency. The analogue-substituted proteins, 4-FW−PE24, 5-FW−PE24, 5-HW−PE24, and 7-AW−PE24, were characterized by absorption and fluorescence spectroscopy. Figure 2A shows the normalized absorbance spectra of native PE24 and the four spectrally enhanced proteins. These spectra were very characteristic of the respective Trp analogue that was incorporated into the protein. The λ_{abs}(max) values ranged from 261 nm (4-FW−PE24) to 283 nm (7-AW−PE24). Notably, 5-HW−

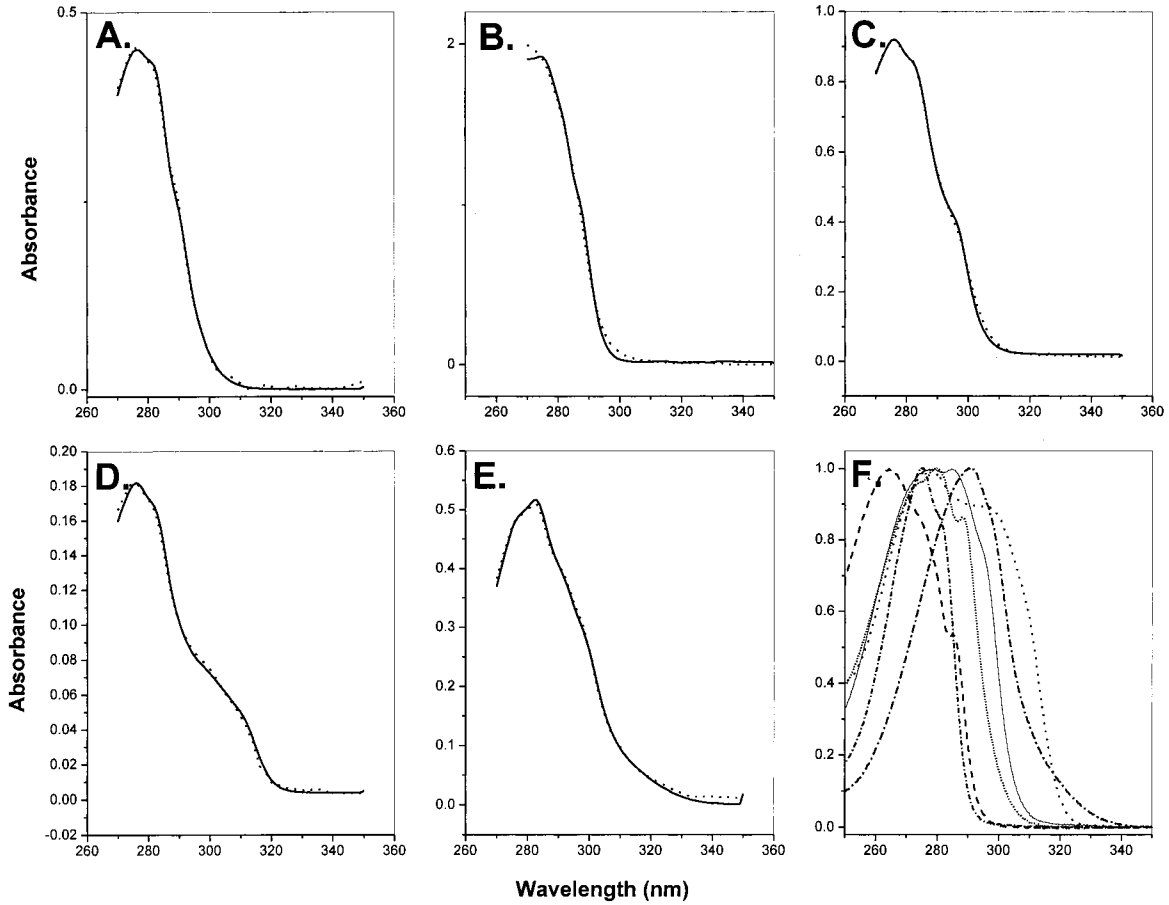

FIGURE 3: Decompose analysis of native and spectrally enhanced PE24 protein absorption spectra. Spectra were arbitrarily scaled and do not reflect relative extinction coefficients. The fits are shown as dotted lines to the spectra (solid lines). Panels: (A) native PE24, (B) 4-FW−PE24, (C) 5-FW−PE24, (D) 5-FW−PE24, and (E) 7-AW−PE24. The absorption basis spectra of the model compounds used for the LINCS analysis fits are shown in (F): 4-FW (dashed line), 5-FW (thin line), 5-HW (dotted line), *t*-Boc (α-amino)-7-AW (dash-dot line), NAYA (fine dot line), and NATA (short dash-dot line). Spectra of model amino acids and proteins were measured in 6 M GdnHCl in 20 mM Tris-HCl and 50 mM NaCl buffer (pH 7.8) at 25 °C.

PE24 exhibited a secondary red-shifted absorption maximum near 300 nm (Figure 2A, dotted line). Also, 7-AW−PE24 showed a significantly red-shifted absorption spectrum compared with that of the native (L-Trp-containing) protein (Figure 2A, dot-dash line). The difference in the absorption spectra between 4-FW−PE24 and 5-FW−PE24 was also interesting, with the former possessing a strongly blue-shifted spectrum (Figure 2A, dashed and thin lines, respectively). The fluorescence excitation spectra are shown in Figure 2B. As expected, these spectra show a correlation with the absorption spectra for the spectrally enhanced proteins but provide an even more characteristic "fingerprint" for the incorporation of the specific Trp analogue. It is noteworthy that the secondary peak for 5-HW−PE24 is more pronounced in the fluorescence excitation scan (Figure 2B, dotted line) than for its corresponding absorption scan (Figure 2A, dotted line).

The fluorescence emission spectra for the native and analogue-incorporated proteins are shown in Figure 2C, and the fluorescence λ_{em}(max) ranged from 332 nm (native PE24) to 379 nm (7-AW−PE24). The fluorescence emission spectra were all normalized (except for 4-FW−PE24) to the same value (1.0 for the respective emission maxima). The apparent quantum yield of 4-FW−PE24 was extremely low, with a weak emission centered near that for the native protein. This weak fluorescence character of 4-FW−PE24 makes it an ideal candidate to study Trp emission from the substrate protein, eEF-2, when acted upon by this spectrally enhanced enzyme. Thus, the incorporation of 4-FW into PE24 renders this protein nearly "spectroscopically silent".

To eliminate environmental differences and all protein structure-induced effects on extinction coefficients for the spectrally enhanced proteins, absorption spectra were obtained when denatured in 6 M GdnHCl (Figure 3). Figure 3A−E shows the absorption spectra of the native and spectrally enhanced PE24 proteins in the denatured state, and the spectra were fit using the Decompose analysis program. The raw spectra are shown in bold with the associated fit shown by a dotted line; it can be seen that the fits were in close agreement with the raw data (Figure 3A−E, residual plots not shown). This spectral-fitting approach provided a rapid measure of quantifying the extent of Trp analogue incorporated into the enzyme. The basis spectra for the model compounds (various blocked Trp analogues) are shown in Figure 3F and were used to calculate the extent of incorporation. The values for the extent of analogue incorporation are shown in Table 1 (AIEs). The extent of incorporation ranged from 82% (5-HW−PE24) to 113% for 4-FW−PE24. The incorporation level for the latter (>100% calculated) reflects the error in this approach to the calculation of the extent of analogue substitution into PE24 by the absorbance fitting method. It was determined that the calculated values were very sensitive to slight changes in the spectrally enhanced

Table 1: Masses and Incorporation Efficiencies of Spectrally Enhanced PE24

protein	calcd MW[a]	obsd MW[b]	AIE (%)[c]
native PE24	24 532	24 535	
4-FW−PE24	24 586	24 580	113 ± 5
5-FW−PE24	24 586	24 592	105 ± 6
5-HW−PE24	24 580	24 584	82 ± 6
7-AW−PE24	24 538	ND[d]	85 ± 4

[a] The calculated molecular weight was obtained by using the program GPMAW, and the mass was calculated using the average isotope distribution for each atom within the PE24 protein. [b] The observed molecular weight was determined by electrospray mass spectrometry (ES-MS) as described in Experimental Procedures. [c] Analogue incorporation efficiencies (AIE) were calculated from the Decompose analysis (see Experimental Procedures) of the denatured protein in 6 M GdnHCl using the appropriate set of basis spectra of the model compounds. [d] Not determined since the error in the ES-MS is greater than the expected difference between the native and the 7-AW proteins.

protein's absorption spectra caused by particle scatter or from UV-absorbing contaminants (nucleic acids, extraneous proteins, etc.).

Mass Spectral Analysis of Spectrally Enhanced Proteins. To provide another measure of the extent of analogue incorporation into PE24, electrospray mass spectrometry (ES-MS) was used, and the mass spectra are shown in Figure 4. All of the proteins, including the native PE24, exhibited a single major peak corresponding to the predicted mass of the protein. The observed (measured) masses of the native and analogue-incorporated proteins (averaged for two or more samples) are listed in Table 1, along with the calculated masses for the native and spectrally enhanced proteins. The ES-MS-determined MW for the native protein (containing a polyHis tag) was 25 434.5 ± 3 Da (six samples) and was in excellent agreement with the calculated mass based on the gene sequence for the protein (24 532 Da). Notably, there was only one major peak (24 534.5 Da, single run) with a minor peak at 24 566.7 Da. The ES-MS values for 4-FW−PE24, 5-FW−PE24, and 5-HW−PE24 were also similar to their respective calculated values, suggesting a high level of analogue incorporation into PE24 at all three Trp sites within the protein, in agreement with the data from the spectral deconvolution method. Furthermore, the mass spectra for the analogue-containing protein samples predominantly showed one peak corresponding to the expected mass for the triple-site-incorporated species. These mass spectral data effectively eliminated the possibility of multiple species existing with no incorporation (24 532 Da), with single-site incorporation (24 550 Da for 4- and 5-FW−PE24; 24 548 Da for 5-HW−PE24), or with two sites replaced with Trp analogues (24 568 Da for 4- and 5-FW−PE24; 24 564 Da for 5-HW−PE24). It was not possible to accurately determine the mass of the 7-AW−PE24 protein by ES-MS since the mass change upon analogue incorporation is too small (24 535 Da for triple-site incorporation) for accurate detection using ES-MS.

Enzymatic Activity of 7-AW−PE24. The enzymatic activity of the four spectrally enhanced proteins was tested and compared with the native PE24. This was accomplished by using a fluorescence-based assay (*19*) that involves ϵ-NAD^+ as the limiting substrate and eEF-2 at saturating levels, and the kinetic data are shown in Table 2. The rectangular hyperbolic nature of the Michaelis−Menten plot for the native PE24 protein indicated that the enzyme follows Michaelis−Menten kinetics (data not shown). A Hanes−Woolf transformation of the WT PE24 kinetic data using least-squares linear regression analysis showed a good fit ($r = 0.998$) with the k_{cat} (1063 ± 15 min^{-1}) and K_M (181 ± 25 μM) values, similar to those reported previously (Table 2; *4*, *19*). The relative k_{cat} activities of the spectrally enhanced enzymes are also shown in Table 2. The 4-FW−PE24 exhibited ADPRT activity that was the most similar to the native enzyme (6-fold lower). However, the 5-FW−PE24 was 26-fold less active than the native enzyme. The 7-AW−PE24 was 53-fold less active, but the least active spectrally enhanced protein was 5-HW−PE24. In the latter case, this reduction in ADPRT activity is similar to that observed when Trps 466 and 558 were replaced with Phe (333-fold reduction, Table 2; *4*). The reduction in catalytic activity could not be attributed to an altered ability to bind the NAD^+ substrate since none of the spectrally enhanced proteins showed variations in their abilities to bind the dinucleotide substrate (Table 2). Furthermore, the 5-HW−PE24 (the least active spectrally enhanced PE24) binds the eEF-2 substrate with a dissociation constant (K_D) near 1000 nM (Figure 6), and this binding constant is similar to the value measured using a FRET assay involving the attachment of extrinsic fluorescence donor (AEDANS) and acceptor (fluorescein) chromophores on PE24 (native) and eEF-2, respectively (S. Armstrong, personal communication). However, NAD^+ binding for the 4-FW−PE24 protein could not be measured using the intrinsic fluorescence quenching assay (since the 4-FW fluorescence intensity was too low for accurate quantification). Notably, the NAD^+ binding of this spectrally enhanced protein was also considered to be similar to the native protein since the ADPRT activity was comparable to that of the native PE24 (Table 2). It is likely that substitution of L-Trp within PE24 with 7-AW or 5-HW causes similar effects to those previously documented when Trps 466 and 558 were replaced with Phe (*4*). These effects were attributed to a minor perturbation of the integrity of the active site geometry (*4*), the impact of which often can be amplified at the level of catalysis (*24*).

Structural Integrity of Spectrally Enhanced Proteins. All of the proteins were tested for their global structural integrity and native fold by proteolysis with dilute trypsin (*4*) (data not shown). Also, the proteins were titrated with urea, and the unfolding profiles were compared with the native protein. These data indicated that both 4-FW− and 5-FW−PE24 proteins were similar in their folded stability to the native protein (data not shown). However, 7-AW−PE24 was less stable, but only slightly. Importantly, 5-HW−PE24 was considerably less stable as evidenced by a more rapid digestion with trypsin and a shift in the denaturation profile to lower urea concentrations (data not shown).

Assay for Binding of eEF-2 with PE24. An assay was devised to measure the binding constant for the eEF-2 and PE24 interaction. This method involved the employment of 5-HW−PE24, in which the 5-HW chromophore can be selectively excited in the presence of the eight Trp residues (L-Trp) located within the eEF-2 protein. Furthermore, the fluorescence emission spectrum of 5-HW−PE24 (Figure 5A) exhibits a large spectral overlap with the absorption spectrum of AEDANS−eEF-2, providing excellent conditions for FRET measurements. The transfer of excitation energy from

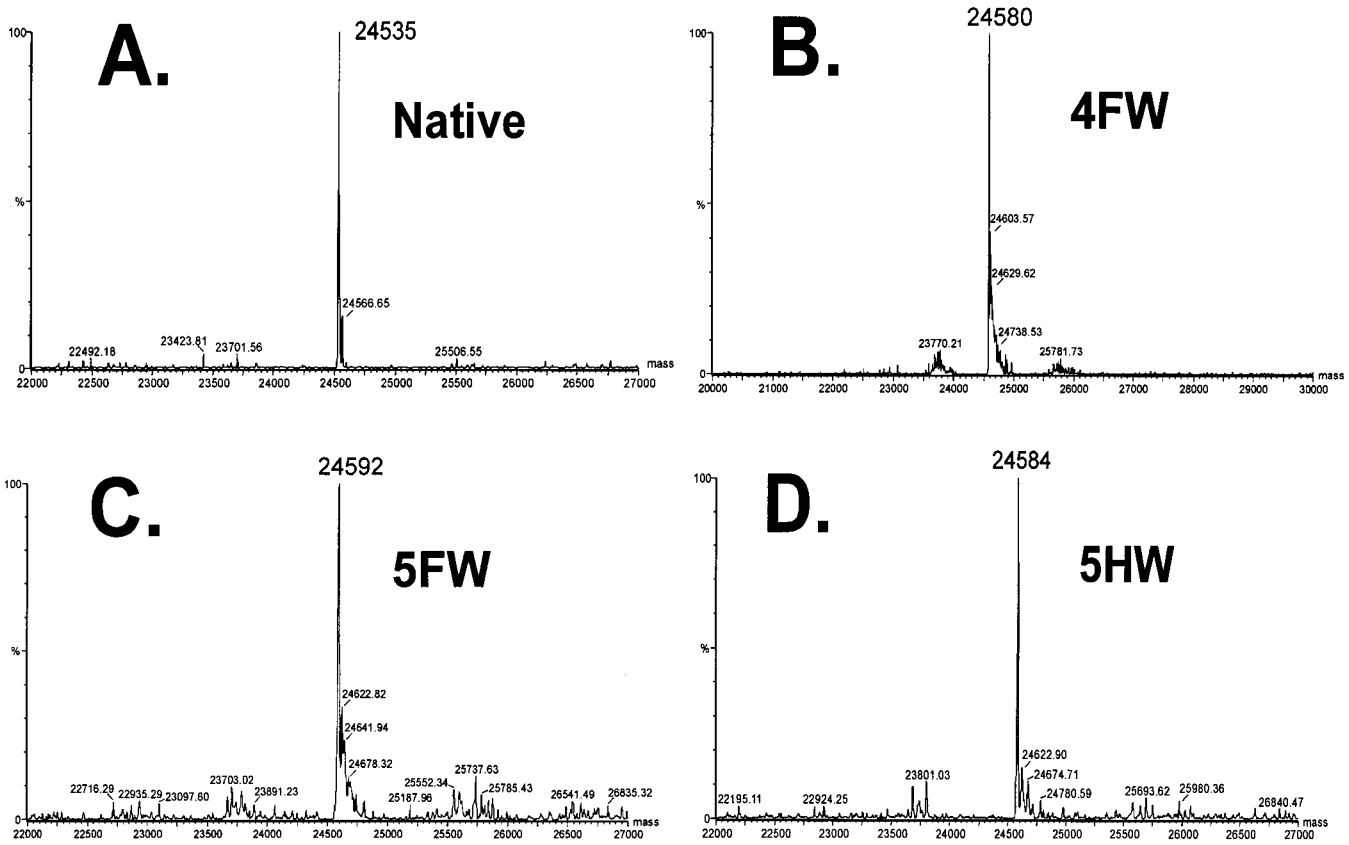

FIGURE 4: Mass spectra of spectrally enhanced PE24 proteins. Panels: (A) native PE24, (B) 4-FW−PE24, (C) 5-FW−PE24, and (D) 5-HW−PE24. The numbers shown on the abscissa correspond to the measured mass in daltons. The proteins were prepared and subjected to mass spectral analysis as described in Experimental Procedures.

Table 2: ADPRT Activity and NAD^+ Binding Affinity of Spectrally Enhanced PE24

protein	relative ADPRT (%)[a]	$K_D(NAD^+)$ (μM)[b]
native	100	38 ± 2
4-FW−PE24	16.7 ± 1.1	ND[c]
5-FW−PE24	3.9 ± 0.4	41 ± 3
7-AW−PE24	1.9 ± 0.1	35 ± 21
5-HW−PE24	0.3 ± 0.05	34 ± 7

[a] The relative ADPRT was calculated by comparing the activity of the various spectrally enhanced proteins with the native PE24 protein. The k_{cat} value for the WT protein was 1063 ± 15 min^{-1} and was determined as described in Experimental Procedures. [b] The NAD^+ binding affinity was determined as described in Experimental Procedures. [c] Not determined.

the 5-HW−PE24 donor to the AEDANS−eEF-2 acceptor was readily apparent upon titration of the donor with acceptor (Figure 5B). The binding of eEF-2 to PE24 resulted in a dose-dependent decrease in the 5-HW−PE24 (donor) fluorescence intensity with the concomitant increase in the fluorescence intensity of AEDANS−eEF-2 (acceptor). The fluorescence intensity of the donor was routinely monitored during the titration of 5-HW−PE24 with AEDANS−eEF-2 to produce binding data curves (Figures 6 and 7).

Determination of Dissociation Constant for eEF-2 Binding to PE24. The binding data for eEF-2 with PE24 are shown in Figure 6. The titration of a 5-HW−PE24 solution with AEDANS−eEF-2 resulted in a saturable binding curve from which the binding constant for the enzyme domain with its protein substrate was determined by fitting the data to a single-site binding model (see Experimental Procedures). It was found that the two proteins bound with nearly identical affinity and behavior in either the presence or absence of the NAD^+ analogue, β-TAD^+ (Figure 6), and the K_D values were found to be 1328 ± 420 nM and 983 ± 63 nM in the presence and absence of β-TAD^+, respectively. These binding constants indicate that the binding energy is higher for the eEF-2 substrate with toxin (33.5−34.3 kJ/mol) than for NAD^+ binding [25.6 kJ/mol (*4*)].

Effect of NaCl on eEF-2 Binding. The effect of salt on the binding of eEF-2 with PE24 was investigated since it was previously shown that the ADPRT activity of the toxin is sensitive to the salt concentration in the assay buffer (*20*). The data shown in Figure 7 indicate that there is a small increase in the binding affinity of the two proteins with increasing salt concentration. Although the effect is small, it is opposite to the effect seen with the enzyme activity of the toxin, where the ADPRT activity is nearly zero at 350 mM salt. This salt effect indicates that hydrophobic interactions, not ionic and electrostatic effects, account for the binding of the catalytic domain of the toxin with its protein substrate and that the inhibition of enzyme activity by high salt is not due to an effect on eEF-2 binding.

DISCUSSION

The low incorporation efficiency of 7-AW into PE24 using the T7 expression system could be caused by several factors. The T7 expression system used for the 7-AW incorporation into PE24 is susceptible to gene leakage. Figure 1A shows that, prior to induction and addition of analogue, there is basal expression of PE24 (7-AW−PE24, 0 h). Thus, a portion

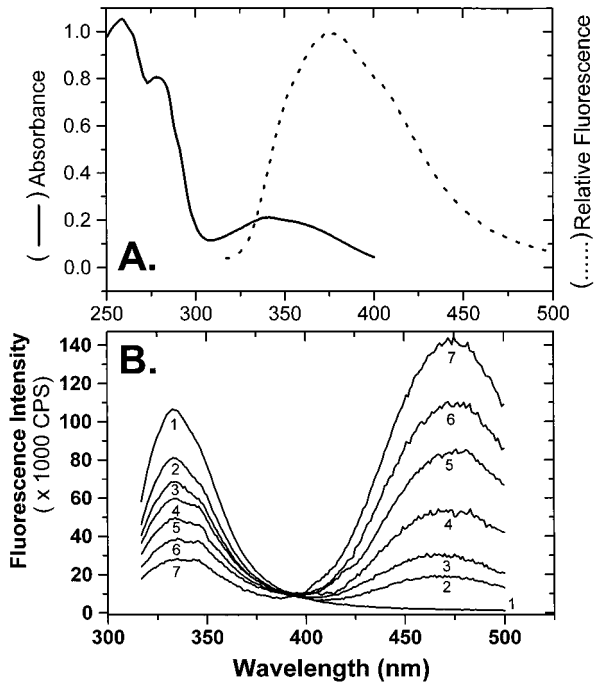

FIGURE 5: Panel A: spectral overlap (FRET) between 5-HW−PE24 (donor, dotted line) and AEDANS−eEF-2 (acceptor, solid line) for the study of protein−protein interactions. The fluorescence emission spectrum of 5-HW−PE24 was acquired as described in Figure 2, and the fluorescence emission maximum was normalized to 1.0. The absorption spectrum of AEDANS−eEF-2 was acquired with a Cary 50 instrument at 25 °C with 1 μM protein concentration in 50 mM NaCl and 20 mM Tris-HCl, pH 7.8. Panel B: titration of 5-HW−PE24 with AEDANS−eEF-2. A solution of 0.5 μM 5-HW−PE24 was titrated with various aliquots of AEDANS−eEF-2 protein solution in 50 mM NaCl and 20 mM Tris-HCl buffer, pH 7.8 at 25 °C. The fluorescence excitation was 310 nm, and the samples were scanned from 317 to 500 nm (4 nm band-passes for excitation and emission).

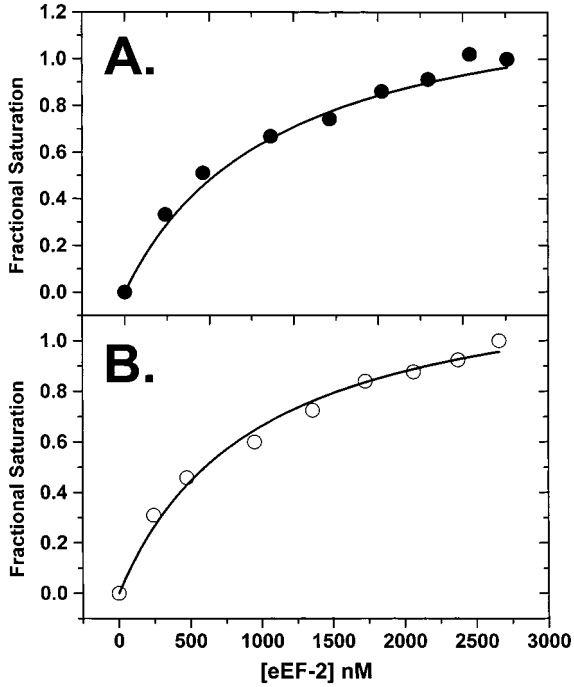

FIGURE 6: Data for binding of AEDANSEnDash−eEF-2 to PE24 in the presence of 200 μM β-TAD$^+$ (panel A) and without β-TAD$^+$ (panel B). The raw data obtained as described in Figure 5 were plotted and fit to the single-site binding function described in Experimental Procedures. The results are representative data for three separate experiments with individual data points repeated in triplicate.

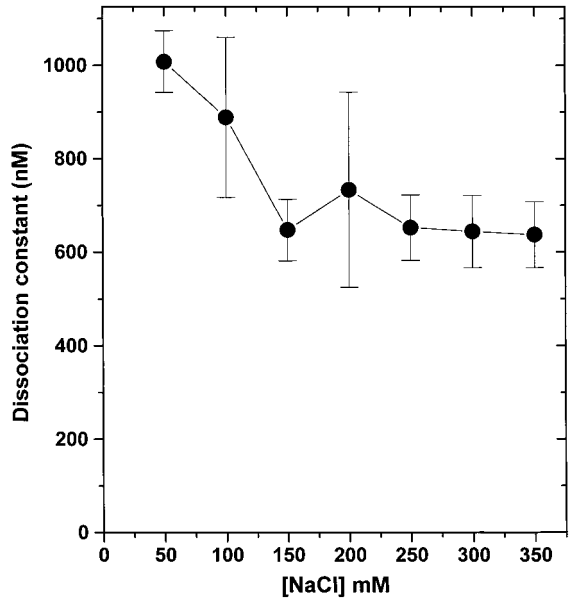

FIGURE 7: Effect of NaCl on AEDANS−eEF-2 binding to 5-HW-PE24. Individual binding experiments were performed as described in Experimental Procedures using various NaCl concentrations in the binding buffer, and the derived dissociation constants were then plotted as a function of the salt concentration used. The experiment was repeated on three separate occasions with the data shown representing the mean ± the standard deviation of three measurements.

of PE24 that is being expressed contains L-Trp and likely contributes to the low incorporation efficiency. However, this basal expression likely cannot account for all 40% of the L-Trp-containing PE24, since there is only approximately 5% leakage inherent to this promoter (*25*). However, the much higher incorporation efficiency found in the *pBAD* expression system effectively rules out some of the possible causes. Importantly, the function of newly synthesized proteins required for protein translation using the T7 promoter may be compromised if an essential Trp residue is replaced in these proteins. Thus, the low efficiency of 7-AW incorporation into PE24 may be explained by the interplay of the different factors described above. Importantly, when the PE24 gene was under the control of the more tightly regulated arabinose promoter, all of the above problems disappeared and provided us with an excellent expression system for analogue incorporation into proteins (Figure 1B, Table 1).

Furthermore, this study has demonstrated that a previously unavailable lysogenic strain of Trp auxotroph can be constructed using a P1 transduction. It was shown that this Trp auxotroph was able to express 7-AW-incorporated PE24; however, a 10-fold reduction in protein yield was observed. This strain was also found to be the most useful one for the incorporation and production of spectrally enhanced PE24 proteins using the *pBAD* expression system (even though the lysogenic properties of the strain are not required for protein induction) perhaps because this strain is also protease deficient, *lon*$^-$. The absorbance and emission spectra of the analogue-incorporated proteins were consistent with those of the model pure analogue compounds, and therefore the product appears to be applicable for the study of toxin−

eEF-2 interactions using intrinsic fluorescence. The report contained in this work illustrates the utility of the *pBAD* expression system for amino acid analogue incorporation using an *E. coli* expression system (*26*). Prior to the present study, the best results to date for analogue incorporation have been obtained by using a *tac* promoter (*13*). Notably, this study demonstrates that there is not selective site incorporation at one or more of the three Trp sites in the toxin but that the extent of analogue incorporation is primarily dependent upon the expression system used.

It is important to determine the extent to which Trp analogues perturb the structure, stability, and function of the protein. Since 5-HW and 7-AW have an additional polar substituent and ring nitrogen atom, respectively (not found in the indole ring), and because Trp residues are usually buried in nonpolar regions of a protein, the expectation is that these Trp analogues may cause some destabilization within proteins. However, in many cases, these analogue-containing proteins retain wild-type function, structure, and stability (*13*, *27*). It is curious that the fluorine-substituted Trp analogues resulted in the most stable proteins, which exhibited the highest analogue incorporation efficiencies and ADPRT activities (Tables 1 and 2). Hydroxyl substitution at the 5-position of indole (5-HW−PE24) caused a noticeable level of protein instability and a 300-fold decrease in enzyme activity.

Wong and Eftink (*27*) investigated the effect of incorporation of 5-HW and 7-AW on protein structure and stability of staphylococcal nuclease. These researchers found that 5-HW did not perturb the folded stability of the nuclease, whereas 7-AW caused a loss in stability. In 1998, the same group investigated further any obvious structural changes upon incorporation of several Trp analogues into the nuclease protein (*28*). They assessed the various Trp analogues including 5-HW, 7-AW, and 4-, 5-, and 6-FW by several techniques. Their results indicated a minimal perturbation of the protein's structure except by 7-AW, which reduced the secondary structure of the nuclease. It was concluded that 7-AW may have a general destabilizing effect on the structure of proteins perhaps because of its polar imino nitrogen at position 7 of the indole ring. Additionally, this polar imino nitrogen has a tendency to H-bond, while the natural environment of an indole side chain of a Trp residue in a protein would not be expected to accept an H-bond at position 7. In contrast, fluorotryptophan analogues showed a slight stabilizing effect on the nuclease protein, which may be due to the properties of the fluorine atom. First, the atomic radius of the fluorine atom is only slightly larger than that of the hydrogen atom. Second, the fluorine atom does not have a strong tendency for H-bonding due to its pronounced electronegativity (*28*). Third, it makes the indole ring more apolar, which will likely favor the nonpolar milieu that Trp residues often occupy in proteins.

The somewhat lower incorporation efficiency of 5-HW and 7-AW into PE24 may simply be due to reduced protein yields found for the respective analogue-incorporated proteins. A lower yield results in more background contamination (extraneous proteins, nucleic acids, etc.), in essence providing a lower signal to noise ratio. The spectral deconvolution method is sensitive to small anomalies (caused by absorption of cellular impurities or particle scattering) in the absorption spectrum of the spectrally enhanced proteins, which can result in a lower calculated incorporation efficiency. The mass spectral data indicated that there was no difference in the amounts of native, single-, or two-site incorporated PE24 proteins in the 5-HW− or 7-AW−PE24 samples as compared with the 4-FW- and 5-FW-incorporated proteins, which suggests that the aforementioned explanation may be valid.

The FRET binding assay for eEF-2 association with PE24 reported herein (Figure 6) is the first account of measuring the binding of these two proteins in solution. The binding constant, near 1 μM, is similar in magnitude to the K_M (eEF-2 substrate) as recently measured by our laboratory (*20*) for the ADPRT activity of PE24. Furthermore, the observation that β-TAD$^+$, a nonhydrolyzable analogue of NAD$^+$, is not required for PE24−eEF-2 complexation is an important one and is in agreement with the recent report of Heggers and co-workers (*29*). Previous data had suggested that the enzyme mechanism is an ordered sequential reaction based on the interaction of immobilized toxin with eEF-2 (*30*) and an ELISA (*31*, *32*). However, the previous binding data involved the immobilization of either the toxin or the eEF-2 protein, which can be misleading if the immobilization procedure causes artifacts. Our own ELISA data (*32*) yielded a K_D for eEF-2 with PE24 near 50 nM, which is 20-fold higher affinity than the solution binding results reported herein. The difference may rest with the immobilization of eEF-2 onto the surface of the microplate well, which prevented catalysis from occurring and may also have resulted in a boric acid (buffer) cross-linked structure/complex that was dependent upon NAD$^+$ as a potential source of alcohol groups for cross-linking (*32*) and may be further compounded by the requirement for antibody to recognize the enzyme−substrate complex. In summary, we believe that the solution FRET binding results contained in the present paper are more physiologically relevant and meaningful. If this is indeed so, then the enzymatic reaction mechanism must be revisited; perhaps, this issue of the mechanism type could be established through the use of product inhibition kinetic experiments.

The effect of salt on the toxin binding to eEF-2 indicates that the well-documented sensitivity of the ADPRT activity of exotoxin A (*33*, *34*) is not due to an effect on the protein−protein interaction between the catalytic domain of the toxin and its protein substrate. The toxin−eEF-2 interaction was surprisingly insensitive to salt over the concentration range studied (0−350 mM NaCl), a range that shows marked inhibition of enzyme activity (*20*). The binding of the NAD$^+$ substrate is also relatively insensitive to salt (*20*). This implies that the ADPRT salt sensitivity stems from ionic interference of catalytic residues during the transferase reaction. It is known that Glu 553 is important for catalysis because of its role in forming an H-bond with the 2′-OH of the nicotinamide ribose of NAD$^+$ (*35*), and it would be expected to be sensitive to high ionic strength in the reaction solution. Also, His 440 is believed to play a role in the transferase step of the ADPRT reaction by possibly interacting with the negatively charged phosphates of NAD$^+$. This interaction would also likely be salt sensitive. Interestingly, both Glu 553 and His 440 (or Arg) are conserved among the various members of the ADPRT family of enzymes, including the eukaryotic PARP enzymes (*36*).

In conclusion, we have demonstrated the feasibility to incorporate the tryptophan analogues 4-FW, 5-FW, 5-HW, and 7-AW into the enzyme domain of ETA and to use this approach to study enzyme−substrate (protein) interactions. We have demonstrated that the *pBAD* expression system is highly regulated and is ideally suited for the incorporation of nonnatural amino acids into proteins using an *E. coli* strain. This system was successful when the previously employed T7 expression system resulted in only 60% analogue incorporation efficiency as judged for 7-AW. Furthermore, the ADPRT reaction catalyzed by PE24 has been proposed to include formation of a binary complex of NAD^+ and toxin, binding of eEF-2 to the binary complex, and transfer of the ADP-ribose moiety of NAD^+ to diphthamide. If the structure and function of the toxin−eEF-2 complex is to be studied using analogues, the ADPRT activity must be blocked; i.e., hydrolysis of NAD^+ must be prevented. Thus, an analogue of NAD^+ is needed in which the N-glycosidic bond to ADP-ribose and nicotinamide cannot be hydrolyzed. The NAD^+ analogue, β-methylenethiazole-4-carboxamide adenine dinucleotide (β-TAD), shows good promise as a substrate, since β-TAD has been crystallized in the presence of PE24 and shows very slow hydrolysis (*2*). Future work in our laboratory is focused on the investigation of the protein−protein interaction mechanism between Trp analogue-incorporated PE24 and eEF-2 during the catalytic cycle of this toxin−enzyme.

ACKNOWLEDGMENT

We thank John Rubinstein for technical assistance and for providing the purified eEF-2 protein for ADPRT measurements. We gratefully acknowledge the assistance of Yolanda Weir in the development of the fluorescence-based ADPRT assay. We are indebted to Dr. J. B. A. Ross for supplying the *t*-Boc-7-AW, for the LINCS program, and for encouragement and helpful discussions during the course of this investigation.

REFERENCES

1. Jinno, Y., Ogata, M., Chaudhary, V. K., Willingham, S. A., FitzGerald, D., and Pastan, I. (1989) *J. Biol. Chem. 264*, 15953−15959.
2. Li, M., Dyda, F., Benhar, I., Pastan, I, and Davies, D. R. (1996) *Proc. Natl. Acad. Sci. U.S.A. 93*, 6902−6906.
3. Bell, C. E., Yeates, T. O., and Eisenberg, D. (1997) *Protein Sci. 6*, 2084−2096.
4. Beattie, B. K., Prentice, G. A., and Merrill, A. R. (1996) *Biochemistry 35*, 15134−15142.
5. Oppenheimer, N. J., and Bodley, J. W. (1981) *J. Biol. Chem. 256*, 8579−8581.
6. Wilson, B. A., Blanke, S. R., Reich, K. A. and Collier, R. J. (1994) *J. Biol. Chem. 269*, 23296−23301.
7. Kessler, S. P., and Galloway, D. R. (1992) *J. Biol. Chem. 267*, 19107−19111.
8. Li, M., Dyda, F., Benhar, I., Pastan, I., and Davies, D. R. (1995) *Proc. Natl. Acad. Sci. U.S.A. 92*, 9308−9312.
9. Galloway, D. R., McGowan, J. L., and Anderson, D. C. (1992) *Pseudomonas aeruginosa* exotoxin A: Immunochemical analysis of the catalytic domain reveals ADPRT toxin cross-reactive isotope, in *Bacterial Protein Toxins* (Witholt et al., Eds.) pp 34−47, Gustav Fischer Verlag, Stutgart.
10. Beattie, B. K., and Merrill, A. R. (1999) *J. Biol. Chem. 274*, 15646−15654.
11. Hogue, C. W. V., Rasquinha, I., Szabo, A. G., and MacManus, J. R. (1992) *FEBS Lett. 310*, 269−272.
12. Ross, J. B. A., Waxman, E., Kombo, B. B., Rusinova, E., Huang, Y. T., Laws, W. R., and Hasselbacher, C. A. (1992) *Proc. Natl. Acad. Sci. U.S.A. 89*, 12023−12027.
13. Ross, J. B. A., Szabo, A. G., and Hogue, C. W. V. (1997) *Methods Enzymol. 278*, 151−190.
14. Laws, W. R., Schwartz, G. P., Rusinova, E., Burke, G. T., Chu, Y. C., Katsoyannis, P. G., and Ross, J. B. A. (1995) *J. Protein Chem. 14*, 225−232.
15. Sambrook, J., Fritsch, E. F., and Maniatis, T. (1989) *Molecular cloning, a laboratory manual*, 2nd ed., Cold Spring Harbor Laboratory Press, Cold Spring Harbor, NY.
16. Silhavy, T. J., Berman, M. L., and Enquist, L. W. (1984) *Experiments with gene fusions*, Cold Spring Harbor Laboratory Press, Cold Spring Harbor, NY.
17. Brent, R. (1992) in *Short Protocols in Molecular Biology* (Ausubel, F. M., Ed.) pp 1−26, John Wiley and Sons, New York.
18. Gill, S. C., and von Hippel, P. R. (1989) *Anal. Biochem. 182*, 319−326.
19. Klebl, B. M., and Pette, D. (1996) *Anal. Biochem. 239*, 145−152.
20. Armstrong, S. A., and Merrill, A. R. (2001) *Anal. Biochem. 292*, 26−33.
21. Gruber, B. A., and Leonard, N. J. (1975) *Proc. Natl. Acad. Sci. U.S.A. 72*, 3966−3969.
22. Steer, B. A., and Merrill, A. R. (1994) *Biochemistry 33*, 1108−1115.
23. Waxman, E., Rusinova, E., Hasselbacher, C. A., Schwartz, G. P., Laws, W. A., and Ross, J. B. A. (1993) *Anal. Biochem. 210*, 425−428.
24. Fersht, A. (1999) in *Structure and Mechanism in Protein Science. A Guide to Enzyme Catalysis and Protein Folding*, W. H. Freeman, New York.
25. Studier, F. W., Rosenberg, A. H., Dunn, J. J., and Dubendorf, J. W. (1990) *Methods Enzymol. 185*, 60−88.
26. Guzman, L. M. (1995) *J. Bacteriol. 177*, 4121−4130.
27. Wong, C-.Y., and Eftink, M. R. (1997) *Protein Sci. 6*, 689−697.
28. Wong, C. Y., and Eftink, M. R. (1998) *Biochemistry 37*, 8947−8953.
29. Elzaim, H. S., Chopra, A. K., Peterson, J. W., Goodheart, R., and Heggers, J. P. (1998) *Infect. Immun. 66*, 2170−2179.
30. McGowan, J. L., Kessler, S. P., Anderson, D. C., and Galloway, D. R. (1991) *J. Biol. Chem. 266*, 4911−4916.
31. Galloway, D. R., Hedstrom, R. C., McGowan, J. L., Kessler, S. P., and Wozniak, D. J. (1989) *J. Biol. Chem. 264*, 14869−14873.
32. Prentice, G. A., and Merrill, A. R. (1999) *Anal. Biochem. 272*, 216−223.
33. Beattie, B. K., and Merrill, A. R. (1996) *Biochemistry 35*, 9042−9051.
34. Carroll, S. F., and Collier, R. J. (1988) *Methods Enzymol. 165*, 218−225.
35. Carroll, S. F., and Collier, R. J. (1987) *J. Biol. Chem. 262*, 8707−8710.
36. Prentice, G. A., Roberts, T. M., and Merrill, A. R. (2001) *Protein Sci. 10* (Suppl.), 409a.

BI011035U